Environmental Research 177 (2019) 108597

Contents lists available at ScienceDirect

Environmental Research

journal homepage: www.elsevier.com/locate/envres

A land use regression model of nitrogen dioxide and fine particulate matter in a complex urban core in Lanzhou, China

Lan Jin[a,*,1], Jesse D. Berman[b,2], Joshua L. Warren[c], Jonathan I. Levy[d], George Thurston[e], Yawei Zhang[c], Xibao Xu[f], Shuxiao Wang[g], Yaqun Zhang[h], Michelle L. Bell[a]

[a] School of Forestry and Environmental Studies, Yale University, 195 Prospect St, New Haven, CT, 06511, USA
[b] Bloomberg School of Public Health, Johns Hopkins University, 615 N Wolfe St, Baltimore, MD, 21205, USA
[c] School of Public Health, Yale University, 60 College St, New Haven, CT, 06510, USA
[d] School of Public Health, Boston University, 715 Albany St Talbot Building, Boston, MA, 02118, USA
[e] Department of Environmental Medicine, New York University, 57 Old Forge Rd, Tuxedo Park, NY, 10987, USA
[f] Key Laboratory of Watershed Geographic Sciences, Nanjing Institute of Geography and Limnology, Chinese Academy of Sciences, 73 East Beijing Road, Nanjing, 210008, China
[g] School of Environment, Tsinghua University, Haidian District, Beijing, 100091, China
[h] Gansu Academy of Environmental Sciences, 225 Yanerwan Rd, Chengguan District, Lanzhou, Gansu, 730000, China

ARTICLE INFO

Keywords:
Land use regression
Vertical variation
$PM_{2.5}$
NO_2
Urban

ABSTRACT

Background: Land use regression (LUR) models have been widely used to estimate air pollution exposures at high spatial resolution. However, few LUR models were developed for rapidly developing urban cores, which have substantially higher densities of population and built-up areas than the surrounding areas within a city's administrative boundary. Further, few studies incorporated vertical variations of air pollution in exposure assessment, which might be important to estimate exposures for people living in high-rise buildings.
Objective: A LUR model was developed for the urban core of Lanzhou, China, along with a model of vertical concentration gradients in high-rise buildings.
Methods: In each of four seasons in 2016–2017, NO_2 was measured using Ogawa badges for 2 weeks at 75 ground-level sites. $PM_{2.5}$ was measured using DataRAM for shorter time intervals at a subset (N = 38) of the 75 sites. Vertical profile measurements were conducted on 9 stories at 2 high-rise buildings (N = 18), with one building facing traffic and another facing away from traffic. The average seasonal concentrations of NO_2 and $PM_{2.5}$ at ground level were regressed against spatial predictors, including elevation, population, road network, land cover, and land use. The vertical variations were investigated and linked to ground-level predictions with exponential models.
Results: We developed robust LUR models at the ground level for estimated annual averages of NO_2 (R^2: 0.71, adjusted R^2: 0.67, and Leave-One-Out Cross Validation (LOOCV) R^2: 0.64) and $PM_{2.5}$ (R^2: 0.77, adjusted R^2: of 0.73, and LOOCV R^2: 0.67) in the urban core of Lanzhou, China. The LUR models for the estimated seasonal averages of NO_2 showed similar patterns. Vertical variation of NO_2 and $PM_{2.5}$ differed by windows orientation with respect to traffic, by season or by time of a day. Vertical variation functions incorporated the ground-level LUR predictions, in a form that could allow for exposure assessment in future epidemiological investigations.
Conclusions: Ground-level NO_2 and $PM_{2.5}$ showed substantial spatial variations, explained by traffic and land use patterns. Further, vertical variation of air pollution levels is significant under certain conditions, suggesting that exposure misclassification could occur with traditional LUR that ignores vertical variation. More studies are needed to fully characterize three-dimensional concentration patterns to accurately estimate air pollution exposures for residents in high-rise buildings, but our LUR models reinforce that concentration heterogeneity is not captured by the limited government monitors in the Lanzhou urban area.

* Corresponding author. Yale School of Forestry and Environmental Studies, 195 Prospect St, New Haven, CT, 06511, USA.
E-mail address: lan.jin@yale.edu (L. Jin).
[1] Present address: Yale School of Medicine, Yale University, 60 College St, New Haven, CT 06511.
[2] Present address: Environmental Health Sciences Division, University of Minnesota School of Public Health, 420 Delaware Street SE, Minneapolis, MN 55455.

https://doi.org/10.1016/j.envres.2019.108597
Received 6 May 2019; Received in revised form 15 July 2019; Accepted 19 July 2019
Available online 22 July 2019
0013-9351/

1. Introduction

Land Use Regression (LUR) models have been widely used in recent air pollution epidemiology studies because they can capture intra-urban air pollution variations at high spatial resolution (Hoek et al., 2008). However, few LUR studies have focused on urban cores, which have substantially higher densities of population and built-up areas than the surrounding suburban/rural areas in a city. An urban core usually accounts for less than 20% of a city's area, but has a population density that is over 10 times higher than that of the surrounding areas in the previous LUR studies (Chen et al., 2010a; Lee et al., 2017; Meng et al., 2015; Wolf et al., 2017). The drastic differences in population density and physical landscapes between the urban cores and surrounding areas might lead to different air pollution sources and dispersions.

Previous LUR models showed different spatial predictors in the urban cores and their corresponding metropolitan areas (including urban cores and suburban/rural areas), even when the same monitoring data or the same candidate predictors were used in Tianjin (Chen et al., 2010a), Hong Kong (Lee et al., 2017; Shi et al., 2016), China, and New York City (NYC) (Ross et al., 2007, 2013), USA. One possible explanation is that the relationships between some spatial predictors and air pollution concentrations might vary by different degrees of urbanicity. At the metropolitan level, comprehensive spatial predictors characterizing the degrees of urbanicity were more likely to be included, while at the urban-core level, specific types of pollution sources or specific land use types were more likely to be identified. In NYC (considered as an urban core) (Clougherty et al., 2013b), truck traffic (a specific type of traffic) was included in addition to traffic-weighted road density in the $PM_{2.5}$ model (Ross et al., 2013), while in the NYC metropolitan area (including surrounding counties), only total traffic was included, and the contribution of truck traffic was not detected, although it was offered as a candidate predictor (Ross et al., 2007). Similarly, in the urban core of Hong Kong (~100 km^2), three traffic-related variables (primary, ordinary road densities, and public vehicles) were included (Shi et al., 2016), while in Hong Kong (1,106 km^2), only expressway length was included as a traffic-related variable in the $PM_{2.5}$ model (Lee et al., 2017). In addition, urban cores were shown to have substantial spatial heterogeneity in air pollution levels (Apte et al., 2017; Clougherty et al., 2013a).

Despite recent advancement in LUR models in China, especially at the national level, most studies used government monitoring data (Barratt et al., 2018; Chen et al., 2018a, 2018b; He et al., 2018; He and Huang, 2018; Xu et al., 2018; Yang et al., 2018; Zhang et al., 2018). The government monitoring network has sparse sampling sites and few sites are near traffic (He et al., 2018; Xu et al., 2018), thus the government monitors are not ideal to capture fine-scale variation of air pollution in a city. To address these challenges, many European or North American studies used purposefully designed monitoring networks to investigate intra-urban variations of air pollution (Beelen et al., 2013; Eeftens et al., 2012; Kanaroglou et al., 2005; Matte et al., 2013). In our pilot study, we found that the limited government monitors (N = 4) did not capture the fine-scale spatial variation of NO_2 in the Lanzhou urban core based on measurements in summer 2015 (Jin et al., 2019). More studies are needed to develop dense monitoring networks and models with high spatial resolution, as they might be crucial to inform local environmental health policies.

Few studies considered vertical variation of air pollution by building height in exposure assessment, which might lead to exposure misclassification for urban areas with dense high-rise buildings (Barratt et al., 2018). To the best of our knowledge, two previous studies incorporated vertical variations in the ground-level exposure models (Barratt et al., 2018; Ho et al., 2015). Barratt et al. measured $PM_{2.5}$ and Black Carbon (BC) at 4 different heights ranging from 0 to 50 m (~20th floor) in 6 locations of Hong Kong, which were used to estimate an average exponential decay rate that was applied to the entire city for derivation of the ground-level LUR model predictions. Ho et al. measured $PM_{2.5}$ at 30 sampling sites with 3 categories of heights (1–3, 4–6, and 7–9 floors) in Taiwan, and the heights were included as a categorical variable in the LUR model. No previous study has estimated vertical variation for NO_2 exposures, which might be very different from $PM_{2.5}$ or BC, given their distinctly different near-road decay patterns (Karner et al., 2010). Furthermore, no study has investigated whether the vertical variations of air pollution differ by the window orientation with respect to traffic, which might lead to exposure misclassification for residents living in an apartment facing away from a street. Our study will be the first to incorporate NO_2 vertical variation in exposure models, to investigate the impacts of window orientation on vertical variations, and to take measurements at shorter intervals vertically up to the 32nd floor in an attempt to more accurately characterize the vertical variations.

In addition, previous studies focusing on vertical dispersions showed a wide range of decay rates: 4%–35% decreases in $PM_{2.5}$ concentrations from the ground level to the 11th floor (Chan and Kwok, 2000; Wu et al., 2002, 2014). These trends relate in part to the local vs. regional source contributions to ground-level concentrations, as well as the built environment and dispersion dynamics. The varying results on vertical profiles of air pollution in different urban settings highlights the need of additional research and for local studies. Our study provided the first observation on vertical variations of air pollution in Mainland China, which have different pollution sources, built environment characteristics, and meteorological conditions than the previous study areas where vertical variations were reported.

This study addresses several research gaps in LUR modeling, and develops LUR models incorporating vertical variations of air pollution in the Lanzhou urban core, in a form that could allow for exposure assessment in future epidemiological investigations.

2. Material and methods

In this study, we investigated the spatial and seasonal variations of air pollution at the ground level and vertical variation by building height, and developed LUR models and predictive models of vertical concentration gradients in the Lanzhou urban core. In our pilot study, we developed a pilot LUR model based on NO_2 measurements at 47 ground-level sampling sites in 2015 summer (Jin et al., 2019). In this study, we will expand our pilot work by adding more sampling sites (75 ground sites and 18 building sites), and sampling more pollutants (NO_2 and $PM_{2.5}$) in four seasons of 2016–2017.

2.1. Study area and spatial data collection

The urban core of Lanzhou is a river valley with the highest population and traffic densities in the city (Fig. 1). The urban core of Lanzhou is shown in the administrative map (Fig. S1). With high mountains surrounding the valley, the atmosphere is usually stagnant, leading to poor air quality in the valley (Zhang and Li, 2011). The urban core includes four administrative districts with various degrees of urbanicity and differing topography: 1) Chengguan District, in the eastern side of the valley that is wider, flatter, and more developed than other districts, with high densities of population, roads and businesses; 2) Anning District, in the north, a relatively new residential area with some industrial sites in the west end of the district; 3) Qilihe District, a hilly area in the south that is under development; and 4) Xigu District, in the west, an industrial area (e.g., power plants and cement factories). Pollution source profiles of particulate matter were reported to vary within the study area; the contribution of traffic was almost 5 times higher in the east than the west, while the contributions of soil dusts and industry emissions were almost twice as high in the west compared to the east (Qiu et al., 2016). Many apartment buildings are more than 30 floors and have mixed window orientation in relation to roadways. Chengguan District has the highest density of high-rise buildings.

We collected spatial information necessary for LUR development,

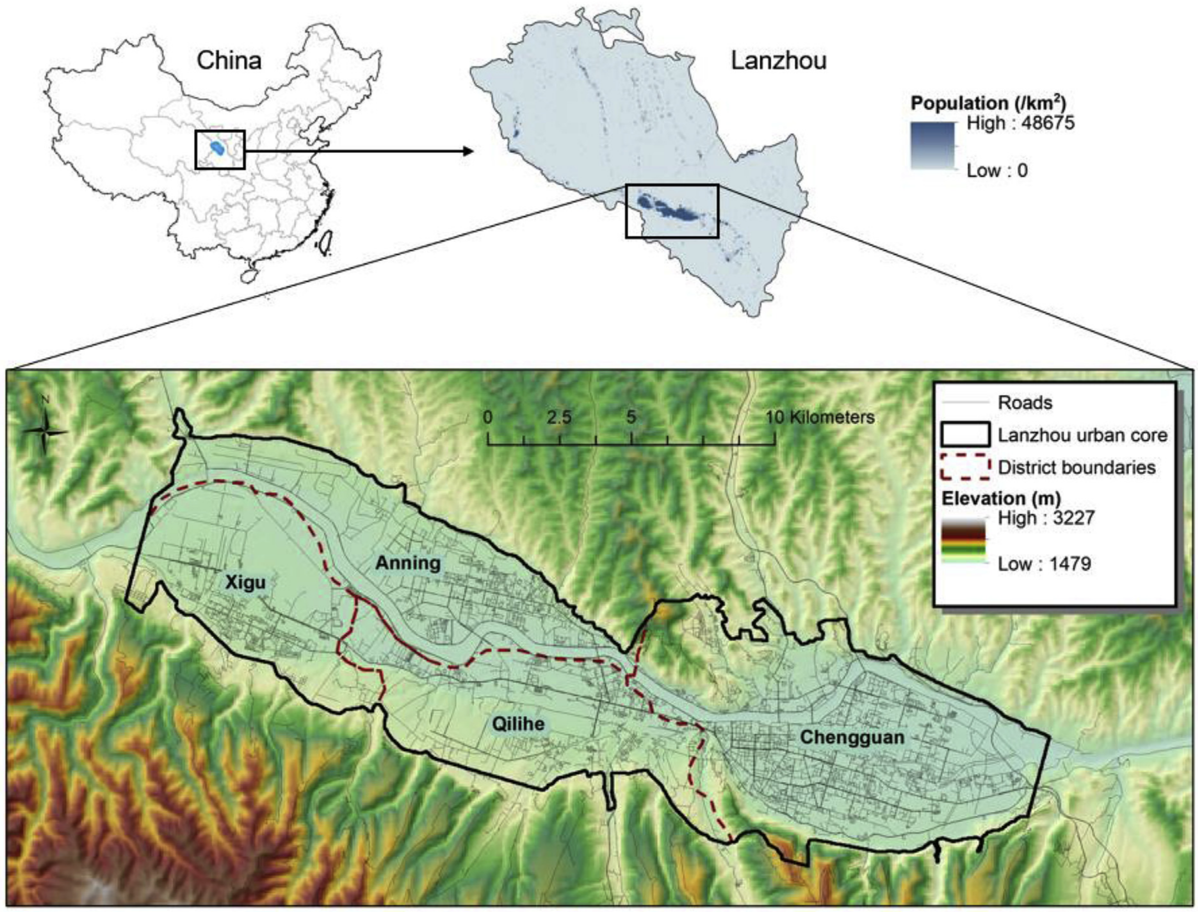

Fig. 1. Lanzhou city and the urban core situated in a valley.

including road network, land cover, land use, elevation and population density. The sources of these datasets were detailed in our pilot study, in which we developed a LUR model for NO_2 based on measurements in a single season at fewer sampling sites compared to this study (Jin et al., 2019). During the sampling campaigns, air pollution concentrations measured by the national regulatory monitoring network and meteorology information were obtained from the China Environment Monitoring Center and China Meteorological Administration.

2.2. Monitoring network design and sampling timeframe

The monitoring network at the ground level includes 75 sampling sites for NO_2 and 38 for $PM_{2.5}$ (Fig. 2). These sites were selected to ensure capturing wide ranges of spatial characteristics and expected air pollution variations. In the pilot study, we selected 47 sampling sites using stratified-random sampling followed by purposeful selection in gaps of spatial coverage and predictor distributions (Jin et al., 2019). Based on the pilot measurements at the 47 sites in 2015 summer, we developed a statistical simulation procedure to select additional 28 sites in areas with low monitor density to improve simulated prediction performance (Berman et al., 2019). The sampling sites for $PM_{2.5}$ are a subset of the sites for NO_2, with all $PM_{2.5}$ measurements collected within 200 m of the NO_2 sampling sites for logistical reasons.

To capture vertical variation in air pollution levels, we took measurements at two selected buildings in residential building complexes (Fig. 2). Monitors were deployed outside the windows of hallways. These windows were facing towards traffic in one building and facing away from traffic in another building. In each building, 9 sites were approximately evenly distributed from the 1st to the 32nd floors (i.e., floors 1, 4, 8, 12, 16, 20, 24, 28, and 32). The heights of the monitors from the ground level were measured using a laser distance measure (Bosch GLM35). The building height was similar between the two buildings where vertical profile measurements were collected. Each floor was ~3-m tall, while the first floor (lobby) was slightly taller than other floors. The vertical decay of $PM_{2.5}$ and BC was reported not to significantly differ by street canyon physical parameters in Hong Kong based on measurements in a wide range of street configurations (i.e., street canyons and open streets, aspect ratios ranging from 1.1 to 7.4, and traffic density from low to high) (Barratt et al., 2018). In this present study, we investigated an aspect of building configurations (window direction in relation to roadways) and its impact on estimated vertical variations of air pollution, which was not considered in previous studies but could be important for evaluating population exposures.

The sampling campaigns for NO_2 were conducted for 2 weeks in each of 4 seasons from 2016 spring to 2017 winter. The specific dates for sampling were selected to be representative based on previous government monitoring data (Henderson et al., 2007). For the winter period, the sampling started 2 weeks earlier than the predetermined date to avoid the Chinese New Year celebration, which usually lasts ~10 days and influences transportation patterns around the celebration time. The final sampling periods at ground level were: 1) April 19-May 3, 2016; 2) July 14-28, 2016; 3) October 14-28, 2016; and 4) January 3-17, 2017. The vertical profile monitors at the buildings were deployed and collected one day after the ground sites. $PM_{2.5}$ was measured at the same time when NO_2 was sampled, but for the vertical profile measurements, $PM_{2.5}$ measurements were only conducted in summer, fall and winter due to logistical challenges (lack of access to the buildings

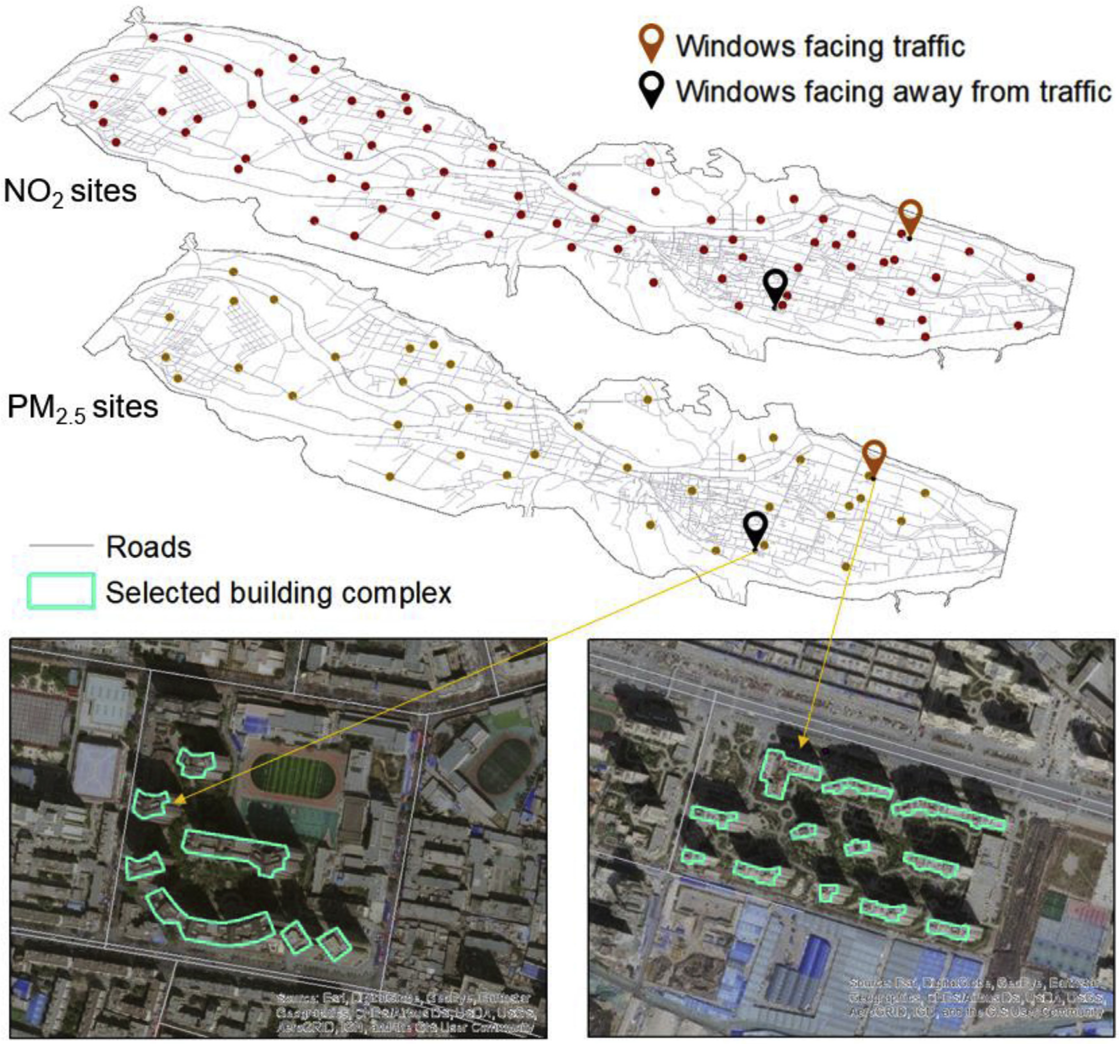

Fig. 2. Sampling sites for NO_2 (N = 75) and $PM_{2.5}$ (N = 38) measurements, including two selected building sites for measuring vertical variation.

during the spring sampling campaign).

2.3. Monitor deployment for NO_2 and $PM_{2.5}$

NO_2 was sampled using Ogawa badges with shelters to avoid sun and rainfall. The microenvironment of potential sampling locations was investigated before installation to ensure the safety of the badges and a free circulation of air around the badges. The badges were installed at least 2.5 m above ground, 30 cm (cm) away from walls at the ground level, and 10 cm from walls at building sites for safety concerns. Field blanks (2 filters) went through the same processes of deployment, transportation and experiment with the samples. The Ogawa badges at the ground level were deployed within 12 h of the first day of each sampling period, and were collected 2 weeks later on the same day. The schedule for deployment and collection of the badges at building sites was a day later than the ground sites. Ogawa pads were analyzed using Ion Chromatography (Demokritou et al., 2001; Gaffin et al., 2017). The measured nitrite concentrations in the extracted solutions were converted to gas concentrations considering the dilution factor and the diffusion coefficient under relative humidity and temperature in the study area during each sampling period.

$PM_{2.5}$ was estimated using measurements from a DataRAM pDR-1000 (Thermo-MIE Inc., Smyrna, GA). This handheld portable device is a passive nephelometer measuring light scatter from fine particles in the range of 0.1–1 μm, which have been shown to be highly correlated with $PM_{2.5}$ mass concentrations measured by gravimetric methods (i.e., Harvard Impactors) (Liu et al., 2002; Quintana et al., 2000). The readings from the monitors were converted to $PM_{2.5}$ mass concentrations based on their established relationship under specific meteorological conditions (Liu et al., 2002).

A mobile strategy was used to collect $PM_{2.5}$ measurements, as there were not sufficient monitors to deploy at all sites concurrently (Larson et al., 2009). Generally, a “mobile” monitor visited each site systematically, and then the measurements were temporally adjusted by government monitoring data or measurements from an “anchor” monitor during the same sampling periods. The “anchor” monitor was the same as the mobile monitor, both of which are the DataRAM pDR-1000 mentioned above. Before deploying in the field, they were both zeroed with Z-pouches. They were also run side-by-side for 30 min before the sampling and showed good agreement (correlation coefficient: 80%). We assume that adjusting for the measurements of the “anchor” monitor can reasonably remove the temporal variations in the measurements of the mobile monitor, allowing for the investigation of variations at different sampling sites measured by the mobile monitor. At the ground level, the “mobile” monitor visited the sampling sites (N = 38) sequentially from 4 to 7 pm on ~5 days in each season. At each sampling site, the “mobile” monitor traced the patterns in Fig. 3 to capture the ambient pollution levels. The “mobile” measurements were adjusted using the following equation: $Adj\ M_i = M_i \times \frac{Ave}{G_i}$, where M_i is the average “mobile” monitor measurements at the i^{th}site, and G_i is the

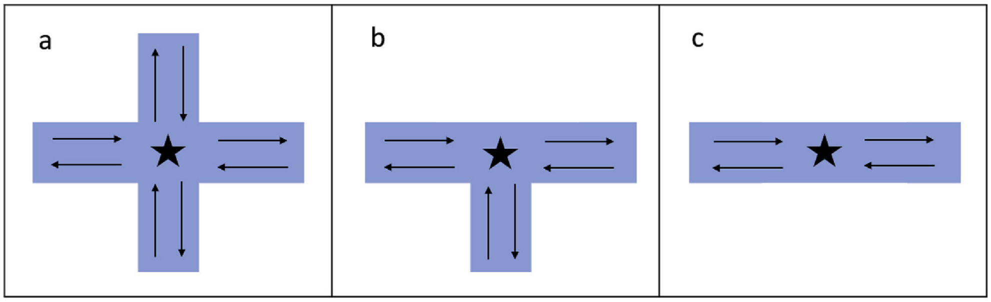

Fig. 3. Mobile monitoring routes at ground sites for $PM_{2.5}$ measurements (a, site that is near a crossroad; b, site that is near a 3-way intersection; c, site that is not near an intersection). Note: The stars represent the sampling sites under different scenarios and an arrow represents 1-min walking distance.

government monitor measurements during the sampling period at the i^{th} site, and *Ave* is the average concentrations of government monitoring data during all sampling periods of a season. For vertical profile measurements, one "mobile" monitor was run for 5 min on each floor, while another "anchor" monitor was run on a fixed floor at the same time. The measurements were conducted during morning rush hours (8:30–9:30 a.m.) and afternoon non-rush hours (2:30–3:30 p.m.) on ~6 days in each season. The mobile measurements were adjusted for temporal changes using the following equation: $Adj\ M_i = M_i \times \frac{\sum_1^{32} A_i / 9}{A_i}$, where M_i is average "mobile" monitor measurements at the i^{th} floor, and A_i is average "anchor" monitor measurements during the sampling period at the i^{th} floor, and $\sum_1^{32} A_i/9$ is the average concentrations in the "anchor" monitor during sampling from the 1st to the 32nd floor ($i = 1, 4, 8, 12, 16, 20, 24, 28, 32$).

2.4. Developing LUR models incorporating vertical variation

The *ground-level* measurements of NO_2 and $PM_{2.5}$ were regressed against spatial predictors to explain variability in air pollution concentrations at the ground level. The development of the spatial predictors was described in our previous work which reported our pilot measurements at fewer sampling sites in one season (Jin et al., 2019). Briefly, a total of 17 categories of variables with buffers up to 2000 m were developed, including an indicator of administrative districts, population density, elevation, land use, land cover, distance to major roads, road density, and restaurant density. A complete list of the spatial predictor variables is provided in Table S1.

Linear regression models were first developed for 6 response variables: annual average NO_2 concentrations, averages of NO_2 concentrations for each season, and annual average $PM_{2.5}$ concentrations. Outliers (> 3 standard deviations away from the mean) as well as void samples due to accidents or errors in deployment or experiment were excluded from subsequent analysis. For some predictors with very skewed distributions, transformations were used. The models were selected using: 1) supervised stepwise selection with adjusted R^2 as the primary criterion, similar to European Study of Cohorts for Air Pollution Effects (ESCAPE) (Beelen et al., 2013; Eeftens et al., 2012), and 2) stepwise selection in both directions using the Akaike Information Criterion (AIC) as the main criterion. Additional criteria for model selection include: 1) coefficients are in the anticipated direction, and 2) p-values for the coefficients are less than 0.2.

For the best model at this stage, assumptions of linear regression models were checked using residual plots. Multicollinearity was assessed using the variance inflation factor (VIF) (James et al., 2013). The model was validated using the leave-one-out cross validation (LOOCV) method, which was shown to be consistent with k-fold cross validation in our pilot measurements. The LOOCV R^2 was computed based on Root Mean Squared Error (RMSE) of prediction at the hold-out sites with the following formula: $1 - (RMSE\hat{}2)/Var(observations)$ (Young et al., 2016). Influential points with high Cook's distance were identified, and excluded to evaluate the improvement of regression models. After excluding an influential point, the model selection procedure was repeated. Additionally, NO_2 concentrations were log-transformed due to a skewed distribution and non-constant variance of the model residuals. The above model selection processes were repeated for log-transformed NO_2 concentrations as a response variable. The residuals of the final model were investigated for spatial autocorrelation using a semivariogram analysis.

Universal kriging models were developed for the 6 response variables (annual average, 4 seasonal averages of NO_2, and annual average of $PM_{2.5}$) using ground level data. The universal kriging models have the following form: $Y(s_i) = \mathbf{x}(s_i)^{\mathrm{T}}\boldsymbol{\beta} + w(s_i) + \varepsilon(s_i),\ \ \varepsilon(s_i) \sim \mathrm{N}(0, \tau^2)$, where $Y(s_i)$ is the air pollution concentration at location s_i (latitude/longitude); $\mathbf{x}(s_i)^{\mathrm{T}}\boldsymbol{\beta}$ is the mean concentration determined by the vector of spatial predictors at location s_i ($\mathbf{x}(s_i)$ are the variables listed in Tables 2 and 3, that are the spatial predictors included in the linear regression models); $w(s_i)$ is a spatially correlated random effect accounting for small scale spatial variability; and $\varepsilon(s_i)$ is independent random measurement error assumed to follow a normal distribution with mean zero and variance τ^2. The spatially correlated random effects are modeled using a multivariate normal distribution, centered at zero, with variance/covariance matrix defined by an isotropic correlation function (i.e., correlation depends only on distance between locations) such that $\mathrm{Cov}(w(s_i), w(s_j)) = \sigma^2\rho(s_i - s_j; \varphi)$ where $\rho(.;\varphi)$ is the selected isotropic correlation function, σ^2 is the variance of the spatial process, and φ describes the strength of spatial correlation in the data. We considered multiple options for $\rho(.;\varphi)$ including the exponential and Gaussian functions (Banerjee et al., 2004; Diggle and Ribeiro, 2007). All models were fitted using the likfit function of the GeoR R package (Ribeiro and Diggle, 2001) where all model parameters were simultaneously estimated using maximum likelihood estimation. Empirical semivariograms were calculated and plotted in order to visualize the spatial correlation in the data and to determine starting values for the model fitting algorithm. The kriging models were compared with the linear regression models based on AIC and LOOCV Mean Squared Error (MSE) for each response variable (annual average, seasonal averages of NO_2,

Table 1
Summary statistics of air pollution concentrations measured by study monitors at 75 monitoring sites for NO_2 and 38 monitoring sites for $PM_{2.5}$ in Lanzhou, China.

Air pollution concentrations (μg/m^3)	Mean	Median	SD	IQR	Min	Max
Annual average NO_2	65.9	62.2	15.7	23.2	42.6	108.2
Spring NO_2	60.4	56.0	16.8	24.3	34.6	101.4
Summer NO_2	57.8	53.6	17.8	27.6	29.9	100.8
Fall NO_2	62.2	61.1	13.5	18.7	39.4	98.4
Winter NO_2	84.0	81.7	17.8	24.9	54.2	135.2
Annual average $PM_{2.5}$	74.7	71.0	18.2	21.0	43.8	112.4

Note: NO_2 was measured during a 2-week period in each season, and $PM_{2.5}$ was measured from 4 to 7 pm in each season.

Table 2
Linear regression model for annual average NO_2 concentrations (μg/m^3; log transformed NO_2 concentrations).

Variables	β	SD	VIF	p-value
Categorical major road[a] density within 100 m (1: ≥75%; 0: < 75%)	0.19	0.042	1.54	< 0.001
Slope (degree)	−0.032	0.0071	1.29	< 0.001
Area of cultivated land within 1000 m (km[b])	−0.10	0.025	1.47	< 0.001
District[b]: Chengguan	0.13	0.042	1.49	0.002
Qilihe	0.10	0.047	–	0.032
Xigu	−0.031	0.057	–	0.592
Major road density within 1000 m (km/km[b])	0.044	0.017	1.06	0.008
All roads density within 100 m (km/km[b])	0.0055	0.0023	1.48	0.020

[a] Major roads are highway, national, provincial, and county-level roads.
[b] The reference of the district variable is Anning District.

Table 3
Linear regression model for annual average $PM_{2.5}$ concentrations.

Variables	β	SD	VIF	p-value
District: Chengguan	−9.6	3.9	1.10	0.020
Qilihe	22	4.9	–	< 0.001
Xigu	−5.1	5.8	–	0.393
Area of industrial land within 2000 m (km^2)	4.5	1.4	1.33	0.003
Average elevation within 2000 m (m)	0.10	0.042	1.09	0.021

Note: The reference of the district variable is Anning District.

and annual average of $PM_{2.5}$).

Vertical profile measurements conducted in the two buildings were plotted against increasing floors (1st- 32nd floors), which were compared between the windows facing toward and facing away from traffic. For NO_2, we investigated the vertical decay patterns of annual average concentrations, and whether the patterns changed across seasons. For $PM_{2.5}$, we investigated the vertical variations of annual average concentrations and whether the variations differed between morning rush hours and afternoon non-rush hours. The vertical variations were characterized using polynomial regression models and exponential models. Exponential models depicting a more rapid decay in the lower floors were applied in previous studies on vertical dispersion (Barratt et al., 2018; Chan and Kwok, 2000; Li et al., 2007; Vardoulakis et al., 2002). Polynomial regression models were also investigated due to their flexibility. The vertical profiles were developed based on both floor numbers and building height. The profile for floor numbers can be useful in exposure assessment because study subjects usually do not know the height of their apartments from the ground, but can easily report their floor. To merge the vertical profiles with the ground-level LUR model, vertical variation functions were proposed to have the following forms. For exponential models, $C_h = C_0\exp(kh)$, where C_h is the air pollution concentration at h m from ground or floor number h, C_0 is the concentration at ground level, k characterizes variations of air pollution with increasing building height which may differ by window directions (if $k < 0$, air pollution decays as building height increases). For polynomial regression models, $C_h - C_0 = \beta_0 + \beta_1 h + \beta_2 h^2 + \ldots + \beta_n h^n$, where $\beta_0 \ldots \beta_n$ are estimated parameters for $h \ldots h^n$. The final model will be selected based on adjusted R^2, AIC and cross-validation MSE.

3. Results

3.1. Summary of air pollution measurements at the ground level

Among the 300 NO_2 samples (75 samples/season * 4 seasons), 5 samples were voided due to accidents (1 lost and 1 broken in spring), deployment error (2 in winter) or experimental error (1 in summer). One outlier was identified in winter measurements (> 3 standard deviations away from the mean). Among the 152 measurements of $PM_{2.5}$ (38 measurements/season * 4 seasons), one outlier was identified in each season except for winter. The voided samples and outliers were excluded from the following analyses. Summary statistics of measured air pollution concentrations are shown in Table 1. NO_2 concentrations in winter were significantly higher than in other seasons ($p < 0.001$). The distributions of annual and seasonal averages of NO_2 and annual average of $PM_{2.5}$ were right-skewed.

The NO_2 concentrations measured by government monitors during the sampling periods showed seasonal patterns consistent with the sampled concentrations (Table S2). The annual averages of NO_2 and $PM_{2.5}$ measured by the government monitors were 10 and 20 μg/m^3 lower than those measured by the study monitors during the sampling periods, respectively. One possible reason for the difference in the concentrations measured by the government and study monitors is the different sampling methods (GB3095-2012, 2012). Near-roadway sites were also oversampled relative to government monitor deployment. Further, ground-level $PM_{2.5}$ was measured by the study monitors in the afternoon from 4 to 7 pm, whereas the government monitors measured daily concentrations, which could contribute to the higher levels observed in the study monitors.

3.2. NO_2 variations at ground level

The coefficients of the final linear regression model for logged

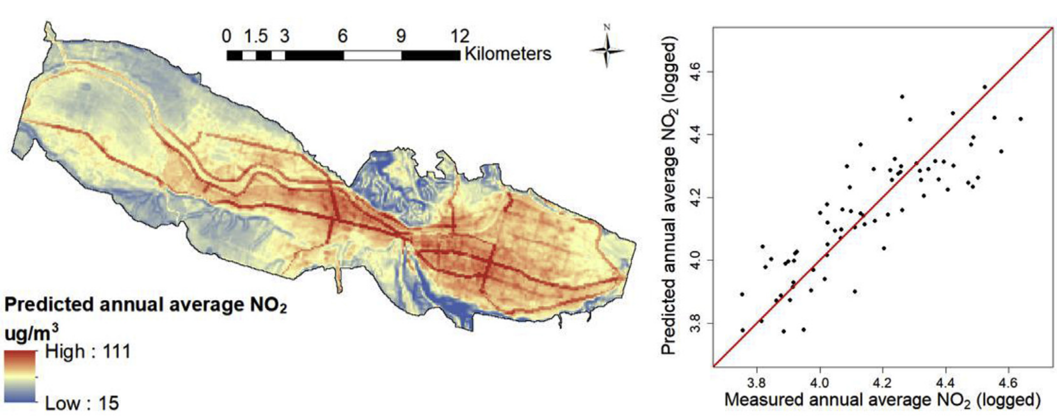

Fig. 4. Predicted annual average NO_2 concentration (μg/m^3) from the linear regression model, and comparison of measured and predicted log average NO_2 concentrations (μg/m^3) at holdout sampling sites. Note: 1) the measurements were from the 75 ground-level sampling sites; and 2) one sampling site was omitted each time to develop a model (against the same set of predictors) to predict the concentration at the omitted site.

annual average NO_2 concentrations are shown in Table 2. The final linear model has an R^2 of 0.71, an adjusted R^2 of 0.67, RMSE of 0.134, and a LOOCV R^2 of 0.64 (Fig. 4). The low VIF values of the final model predictors indicate a lack of multicollinearity. The residual plots and marginal plots show that the model was a good fit for predicting annual average NO_2 (Figs. S2 and S3). Three influential observations with highest Cook's distance were excluded due to substantial improvement in the model fit.

Annual average NO_2 concentrations were significantly higher in the Chengguan and Qilihe Districts, compared to the Anning District. NO_2 concentrations significantly decreased with increasing slope or area of cultivated land. The cultivated land variable was developed based on land cover categories by GlobeLand30 (Chen, 2010; Jun et al., 2014). NO_2 concentrations were positively associated with multiple predictors of road density, which characterized different aspects of the road network and their impacts on the distribution of traffic pollution (Fig. S4). The predicted annual average NO_2 concentrations are mapped in Fig. 4. The range of predicted annual average NO_2 concentrations was 96 μg/m^3, consistent with the measurements across the 75 sampling sites (Table 1) and much higher than the range of measurements from the 4 government monitors (9.5 μg/m^3).

Fig. 5 shows that after controlling for the spatial predictors, the degree of spatial correlation among the NO_2 measurements decreased substantially (effective spatial range decreased from 2404 to 766 m). The covariance parameter estimates (determining the shapes of semivariograms) with and without controlling for the spatial predictors are shown in Table S3. The flat semivariogram with controlling for the spatial predictors indicates an absence of residual spatial autocorrelation in the linear model. While the coefficient estimates of the spatial predictors were similar between the linear regression and universal kriging model (Table S4), the linear model performed better based on its lower AIC (−82.8) and lower LOOCV MSE (0.0180), compared to the universal kriging model (AIC: 79.2, LOOCV MSE: 0.0183).

The spatial patterns of NO_2 were similar across seasons with the highest concentrations in winter (Fig. 6). The models for seasonal averages of NO_2 showed similar prediction performance with slightly lower cross-validation R^2 (Table S5). The predicted and measured NO_2 concentrations were highly correlated in all seasons with correlation coefficients ranging from 0.74 to 0.85 (Fig. S5). The strongest predictors for all seasons are area of cultivated land and major road density within 100 m ($p < 0.05$). District indicator was also included in all seasonal models ($p < 0.2$), but it was a stronger predictor in summer and winter ($p < 0.05$). Area of industrial land was a significant predictor only in winter ($p < 0.01$).

3.3. p.m.$_{2.5}$ variations at ground level

The final model for $PM_{2.5}$ is shown in Table 3. The final model has an R^2 of 0.77, adjusted R^2 of 0.73, RMES of 9.6, and LOOCV R^2 of 0.67 (Fig. 7). The VIF values of the predictors indicate no multicollinearity issues. $PM_{2.5}$ concentrations were substantially higher in the Qilihe District than other districts. The area of industrial land within 2000 m and average elevation within 2000 m were associated with increased $PM_{2.5}$ concentrations. The predicted $PM_{2.5}$ concentrations for the linear model are shown in Fig. 7.

After adjusting for the spatial predictors (in Table 3) the spatial correlation in the measurements decreased substantially: effective spatial range decreased from 4744 to 598 m. The semivariograms and covariance parameter estimates with and without adjusting for spatial predictors are shown in Fig. S6 and Table S3. The flat semivariogram of the universal kriging model indicates an absence of spatial autocorrelation in residuals of the linear regression model. While the coefficient estimates of the spatial predictors were similar between the linear regression and universal kriging model (Table S6), the linear model (AIC: 259; LOOCV MSE: 92.9447) performed slightly better than the universal kriging model (AIC: 263; LOOCV MSE: 92.9448).

The residual plots and marginal plots showed a good fit with the data for the linear regression model (Figs. S7 and S8). Three influential points with the highest Cook's distance were excluded due to substantial improvement in the model fit. Two out of the three influential points were located near construction sites, but spatial data to characterize all the construction sites in the city are unavailable, thus the model underestimated the $PM_{2.5}$ concentrations at these two locations.

3.4. Vertical variations of NO_2 and $PM_{2.5}$ concentrations

The vertical variations of NO_2 and $PM_{2.5}$ differed by window orientation with respect to traffic, and also showed temporal differences. For windows facing traffic, the NO_2 estimated annual average concentrations decreased 18% from the 1st (3.2 m) to the 32nd floor (124.2 m). A significant decrease in the estimated annual average NO_2 concentrations with increasing height was observed for windows facing traffic (p: 0.002), but not for windows facing away from traffic (p: 0.167) (Fig. 8). The final models for vertical decay patterns of NO_2 represent exponential forms due to their lower AIC and cross-validation MSE (Table 4). Despite higher R^2, polynomial regression models showed high cross-validation prediction error especially for more flexible models (with higher degrees of freedom), indicating overfitting the data (Fig. S9). The vertical variations in NO_2 showed seasonal

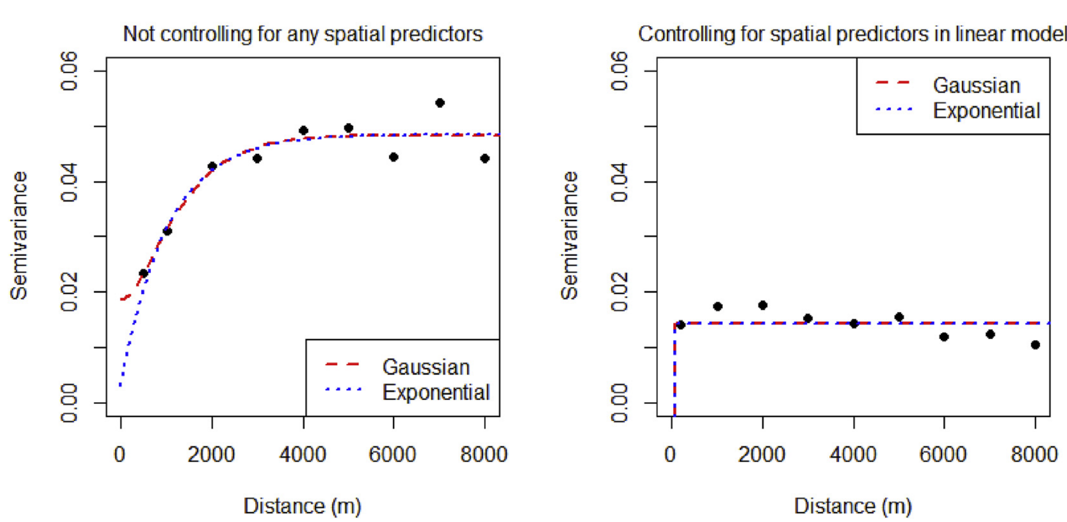

Fig. 5. Semivariograms of annual average NO_2 concentrations (logged) with and without controlling for spatial predictors included in the linear models.

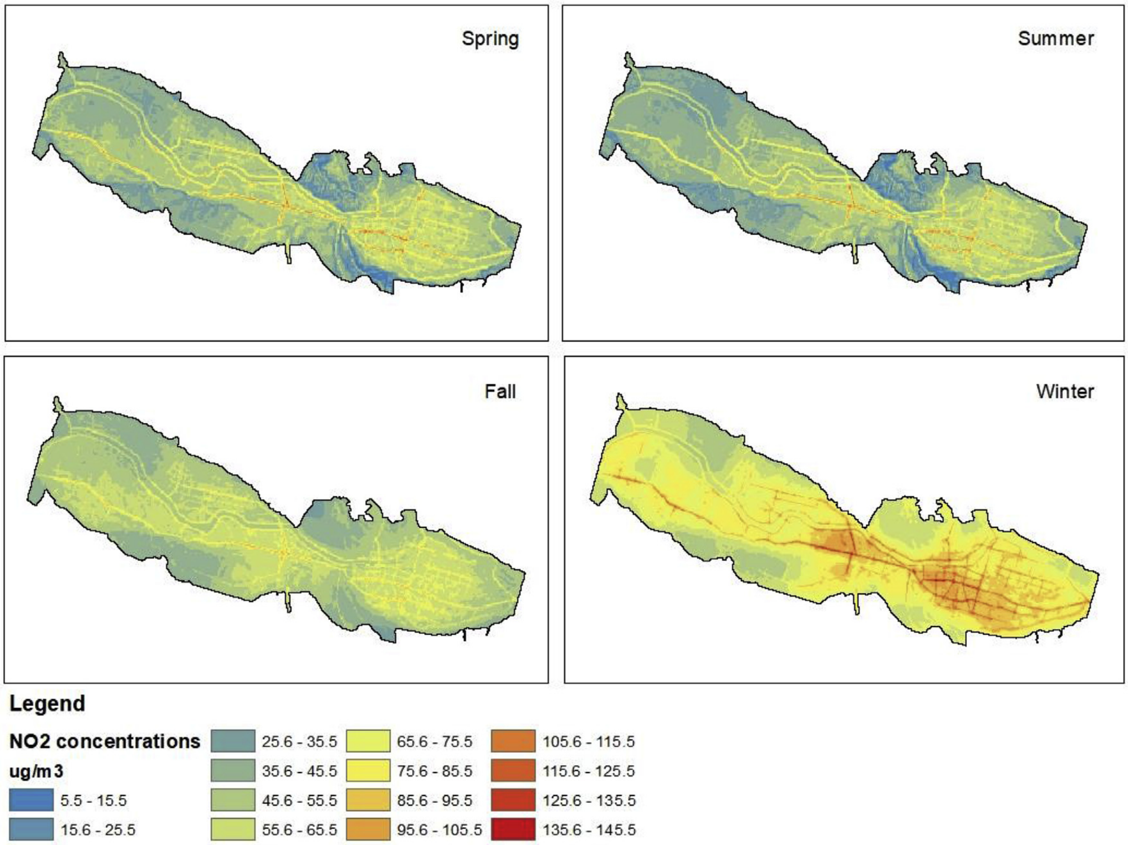

Fig. 6. Seasonal averages of NO_2 concentrations (μg/m^3) predicted by linear regression models.

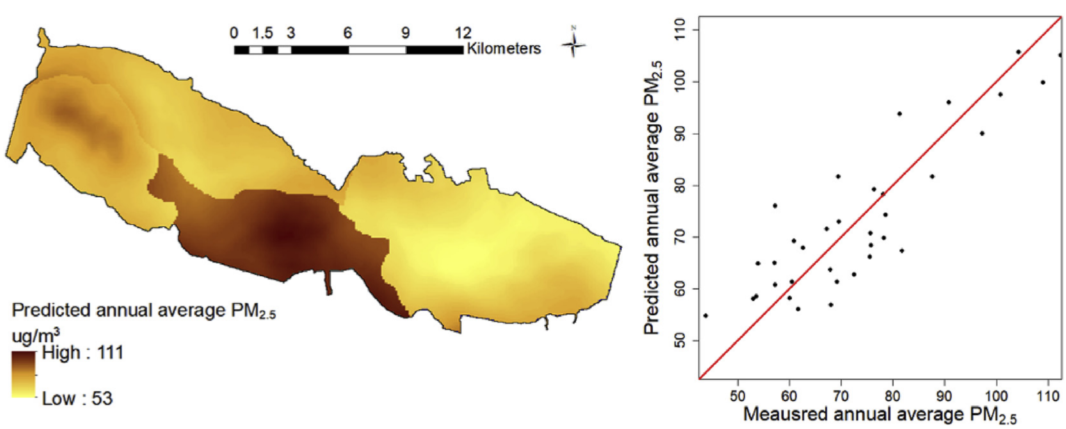

Fig. 7. The predicted annual average $PM_{2.5}$ concentrations (μg/m^3) from the linear regression model, and comparison of measured and predicted annual average $PM_{2.5}$ concentrations (μg/m^3) at holdout sampling sites. Note: 1) the measurements were from the 38 ground-level sampling sites; and 2) one sampling site was held out each time to develop a model (against the same set of predictors) to predict the concentration at the holdout site.

patterns (Fig. 8). In general, winter had the highest concentrations while summer had the lowest concentrations. For windows facing traffic, the vertical decay rate was lowest in winter ($k = -0.002$ per floor) compared to $k = -0.011$, -0.008, and -0.007 for spring, summer and fall, respectively. Fall and winter measurements showed similar fluctuation patterns along the estimated decay trends with higher fluctuations in winter.

A significant decrease in annual average $PM_{2.5}$ concentrations with increasing height (i.e., floors or building height) was observed for windows facing away from traffic (p: 0.016), but not for windows facing traffic (p: 0.853), which contrasts with NO_2 models (Fig. 9). Similar to NO_2, exponential $PM_{2.5}$ models showed the best fit. For windows facing away from traffic, the $PM_{2.5}$ annual average concentrations decreased 9.3% from the 1st (2.1 m) to the 32nd floor (114.1 m). For both window directions, the $PM_{2.5}$ concentrations in the morning rush hours significantly decreased with increasing height at a similar decay rate (Fig. 9). Decay rates were similar between summer and winter ($k = -0.006$), but an increasing trend of $PM_{2.5}$ with increasing height was observed for windows facing traffic in fall (Fig. S10).

4. Discussion

In this study, we found substantial spatial variation of NO_2 and

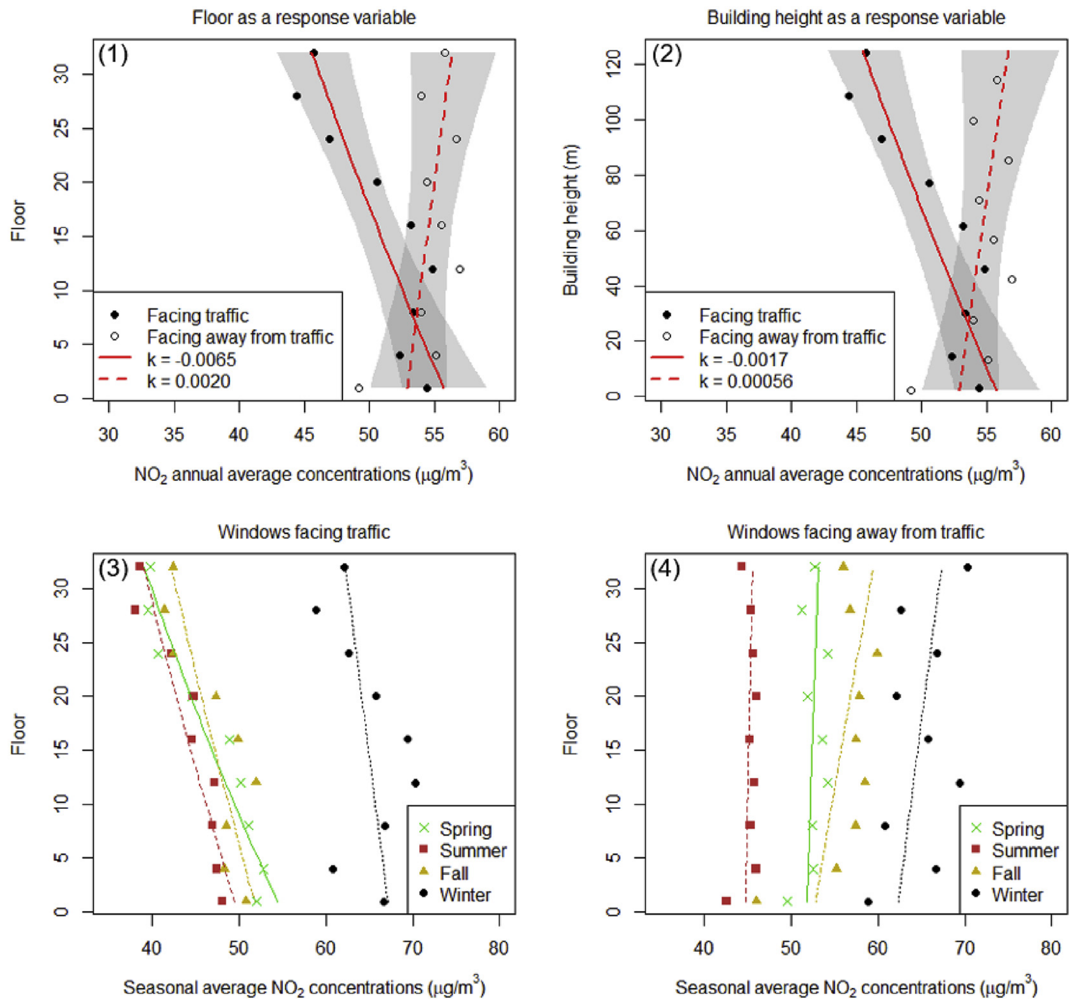

Fig. 8. Vertical measurements and fitted exponential models for NO_2 annual average concentrations (panels 1 and 2), and seasonal changes of vertical variations of NO_2 annual average concentrations (panels 3 and 4). Note: k is the decay rate in an exponential model (Section 2.4), and gray areas are 95% confidence intervals.

$PM_{2.5}$ concentrations predicted by the LUR models across different seasons, while limited government monitors showed little spatial variation in the pollution levels in Lanzhou urban core. Using the LUR models might improve exposure assessment in future air pollution epidemiology studies in Lanzhou, compared to using government monitors alone.

The final LUR models were a good fit for the measurements, explaining 71% and 77% of the variance in the measured NO_2 and $PM_{2.5}$ in this study area, respectively, which were higher than the explained variance by the LUR models developed in the other 2 Chinese urban cores: 51% for an NO_2 model in Changsha, and 63% for a $PM_{2.5}$ model in Hong Kong (Liu et al., 2015; Shi et al., 2016). The explained variance in this study were within the general ranges of R^2 in previous LUR studies worldwide: 0.54–0.92 for NO_2, and 0.49–0.89 for $PM_{2.5}$ (Beelen et al., 2013; Chen et al., 2010a, 2010b; Clougherty et al., 2008; Cordioli et al., 2017; Eeftens et al., 2012; Gilbert et al., 2005; Huang et al., 2017; Lee et al., 2014, 2017; Meng et al., 2015; Rahman et al., 2017; Ross et al., 2006, 2013; Shi et al., 2017; Wolf et al., 2017; Wu et al., 2015). We found that linear regression models performed slightly better than universal kriging models in this study area, which is consistent with low spatial autocorrelation (Moran's I) in the model residuals in some previous studies (Chen et al., 2010b; Cordioli et al., 2017; Lee et al., 2017; Meng et al., 2015; Wu et al., 2015). However, this finding contrasts to air pollution predictions at the continental level in some studies, where universal kriging outperformed LUR models across mainland China, contiguous US, and the European Union (Beelen et al., 2009; Young et al., 2016; Zhang et al., 2018). This difference in performance may be partially explained by the broader geographic coverage of the predictions in these studies.

The distribution of predicted NO_2 concentrations closely followed the road networks in the study area. In the final LUR models for NO_2, three traffic-related predictors were included to characterize the impacts of different aspects of road networks on NO_2 concentrations. Area of cultivated land within 1000 m was significantly associated with

Table 4
Comparisons of models for vertical decay of NO_2 estimated annual average concentrations with increasing floors.

Models	Adjusted R^2	AIC	LOOCV MSE	3-fold cross validation MSE
Exponential	0.732	−28.093	0.002	0.002
Polynomial (df = 2)	0.804	39.924	6.875	10.912
Polynomial (df = 3)	0.822	39.443	14.538	29.216
Polynomial (df = 4)	0.985	16.913	1.834	384.154

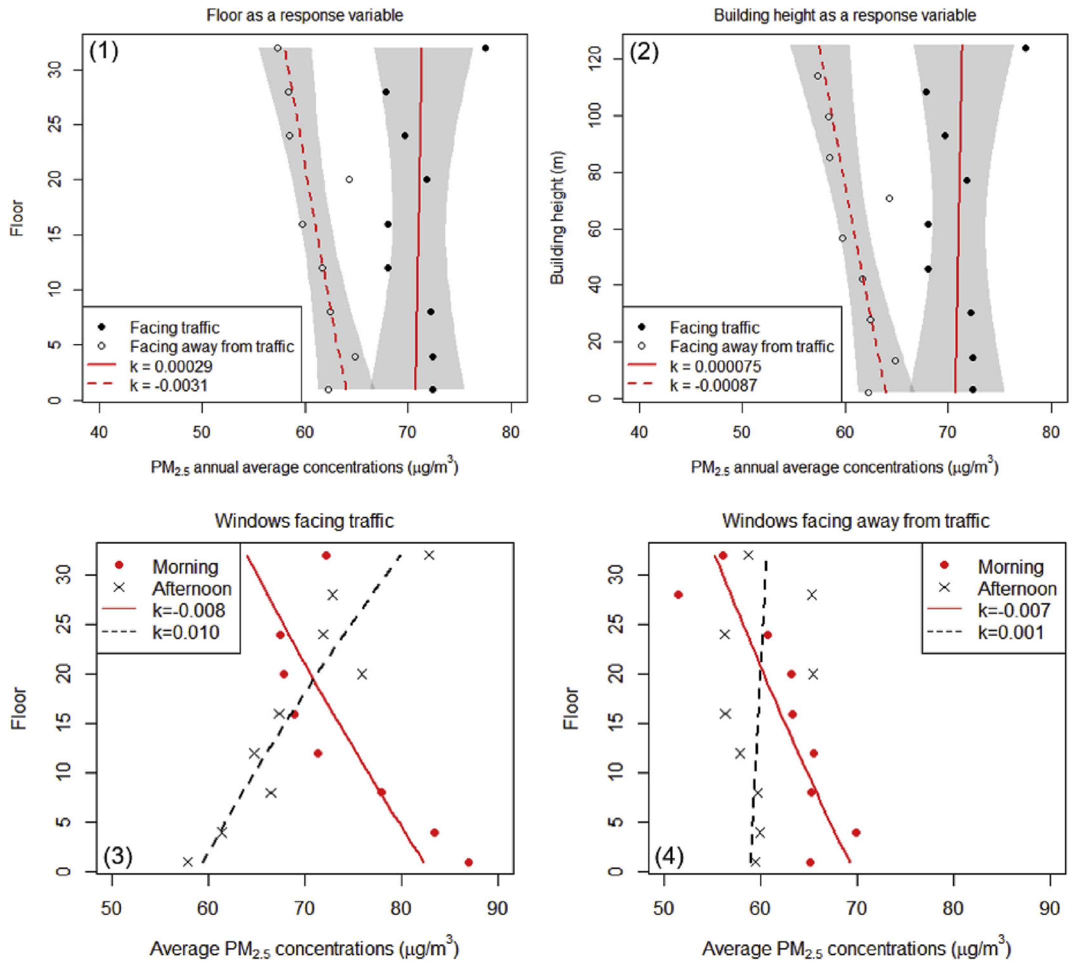

Fig. 9. Vertical measurements and fitted exponential models for $PM_{2.5}$ annual average concentrations (panels 1 and 2), and vertical variations of average $PM_{2.5}$ concentrations in the morning rush hours and in the afternoon non-rush hours (panels 3 and 4). Note: k is the decay rate in an exponential model (Section 2.4), and gray areas are 95% confidence intervals.

lower NO_2 levels, which was not observed in our pilot study with a subset of the sampling sites in this study (N = 47) (Jin et al., 2019). Compared to the pilot study, this study included additional sampling sites in areas on the edges of the city, where more cultivated lands were located. The range of the predictor for cultivated land (area of cultivated land within 1000 m buffer) at the sampling sites (N = 75) in this study doubled that in our pilot study at 47 sites (Fig. S11). This demonstrates the importance of purposeful design of monitoring networks for fine-scale LUR models.

The distribution of predicted annual average $PM_{2.5}$ showed different spatial patterns than NO_2 in the study area. The indicator of administrative districts was the most significant predictor with the highest effect estimates in the $PM_{2.5}$ model. Compared to Anning District (a newly developed residential district), Qilihe District had significantly higher predicted $PM_{2.5}$ concentrations, which could be driven by the development of a High-tech Industrial Development Zone in this district. This Development Zone (~8 km^2) was located in a flat isolated area on a hill. For its development, a series of construction sites have been developed for building high-tech industrial parks, business centers and related residential buildings since 2010 (Li and Deng, 2009). Construction was ongoing during the sampling campaigns. No spatial information was available to accurately depict the specific spatial area of the development zone. The lack of detailed spatial information on the development in Qilihe District might be the reason why the district indicator was the strongest predictor in the $PM_{2.5}$ LUR model, thus the $PM_{2.5}$ prediction surface shows discontinuities. However, we believe that our $PM_{2.5}$ LUR model can capture the spatial variations in $PM_{2.5}$ exposures in the study area; and more importantly, the model is informative for the local government, allowing it to effectively allocate resources for controlling $PM_{2.5}$ in the most polluted area. In addition, the modeling framework being used in the present study can incorporate finer scale spatial information, if it becomes available in the future.

Similarly, different patterns between $PM_{2.5}$ and NO_2 were also reported in other Chinese cities (Huang et al., 2017; Lee et al., 2017). In contrast, predicted $PM_{2.5}$ and NO_2 showed similar patterns in NYC, where a high-to-low gradient was shown from the central borough of Manhattan to the surrounding boroughs (Ross et al., 2013). Our finding that the $PM_{2.5}$ distribution was more spatially homogeneous than NO_2 is consistent with some previous studies (Huang et al., 2017; Lee et al., 2017; Wolf et al., 2017), as NO_2 has fewer regional sources and is dominated by local combustion sources.

Our finding that vertical variations of air pollution differed by windows orientation with respect to traffic, to the best of our knowledge, has not been previously investigated. Unlike some studies reporting that fine particles decreased more rapidly in the first 20 m above the ground and then reached background level by complete mixing (Barratt et al., 2018; Wu et al., 2014), we found continuous decay trends until ~120 m (32nd floors) for windows facing away from the traffic. This could relate to the atmospheric conditions not favoring vertical mixing of air pollution in the valley. Temperature inversions generally occur in the morning in the valley, which can trap air pollution near the ground (Chu et al., 2008), contributing to the significant vertical decay in air pollutant concentrations observed in the morning, but not in the afternoon. As few buildings in the study area have mechanical ventilation systems to circulate fresh air, residents tend to open the windows for ventilation, leading to potential infiltration of outdoor pollution into the indoor environment. Ignoring vertical variations of air pollution could lead to exposure misclassification.

Significant vertical decays of pollution occurred on the side of the building facing traffic for NO_2 and the side facing away from traffic for $PM_{2.5}$. One possible explanation is that NO_2 and $PM_{2.5}$ had different primary pollution sources in the study area, contributing to varying dispersion patterns (especially the air flows near buildings). NO_2 measured by the study monitors is mainly related to traffic in this study area (Jin et al., 2019). Ground-level pollution sources have major effects immediately downwind, and the dispersion of ground-level pollution is most affected by surface features like buildings (Lippmann et al., 2003), which could explain why we observed NO_2 decay at the building side directly facing downwind direction of a busy road, but little vertical variation of NO_2 for the building side that is not directly exposed to traffic. On the other hand, $PM_{2.5}$ was not associated with traffic predictors, but was associated with industrial land use and was the highest in the Qilihe District with large-scale construction on high hills. Industrial emissions from tall stacks or soil/construction dusts from higher elevation can be transported by airstreams travelling long distance. When these airstreams encounter a building, a displacement zone can occur in front of the building, and the airstreams become more turbulent, and create a cavity behind the building, where air pollution can be enveloped and mixed (Lippmann et al., 2003). This might explain the significant decay for the building side facing away from traffic (behind other buildings), but not the building side facing an open street canyon. This differs from a study of the Hong Kong urban area where the $PM_{2.5}$ distribution was associated with traffic predictors at the ground level and significant vertical decrease of $PM_{2.5}$ was observed on the traffic side of buildings (Barratt et al., 2018; Shi et al., 2017). Further research is warranted to explore the observed unexpected increasing trends of $PM_{2.5}$ for afternoon hours in fall (significant at the building side facing traffic). One possible explanation is that under certain meteorological conditions, a stable atmosphere layer trapping air pollution can occur at an elevated height (Lippmann et al., 2003), potentially contributing a measured inverse vertical gradient of air pollution. We found significant difference in vertical variations by window directions and time of the day, indicating the importance and complexity of incorporating vertical variations in population exposures.

An advantage of this study over earlier LUR research is the systematic selection of sample size and locations in the monitoring network design based on distributions of potential spatial predictors and statistical simulation (Berman et al., 2019). This work builds on a pilot study, which ensures that sampling sites have good spatial coverage and capture the gradients of spatial predictors in the study area (Jin et al., 2019). Furthermore, an evaluation of variograms by season revealed little parametric variability based on nugget to sill ratios, indicating monitor locations suitable for assessing year-long concentrations. Near-road decay trends observed in our pilot study ensured the selection of relevant buffer sizes of traffic-related predictors (Jin et al., 2019). Another innovative component of this study is the investigation of vertical variations of air pollution by building height.

$PM_{2.5}$ concentrations at the ground level were measured during the daytime, which does not reflect nighttime exposures as would continuous measurements. More broadly, we had a limited number of sampling days and hours per day for $PM_{2.5}$ measurements, given equipment limitations. That said, our "anchoring" strategy ensured that we were capturing spatial rather than temporal variability, and our LUR models were physically interpretable. The vertical measurements of $PM_{2.5}$ were not conducted in spring due to a lack of access to the buildings at the time. Although we obtained the spatial data that were most closely matching the study period, the land use data from 2005, land cover and major point sources data from 2010 are much older than the monitoring data. Future studies with more recent spatial data can potentially improve prediction performance of the models. In addition, meteorological data were only available for one site in the city and thereby do not provide information on spatial variations; thus, meteorological data were not included in models for annual averages of NO_2 or $PM_{2.5}$. Wind-related meteorological predictors have been suggested to improve LUR models (Shi et al., 2017); however, the wind speed in the study area was low; the average wind power during sampling campaigns was 1.3 (< 1.5 m/s) on a scale of 0–17. Another limitation is the lack of detailed spatial information on construction. Large construction sites were observed during sampling campaigns, but no detailed spatial data were available to identify these sites as a spatial predictor in the model. Additionally, data on traffic volume or vehicle types were unavailable. Finally, future work could examine vertical variations at additional sites; vertical measurements were only measured in two selected buildings.

This study focused on developing LUR models for the urban core of Lanzhou. We hypothesized that the models for urban cores might differ from the models for their larger metropolitan areas because the relationships between some spatial predictors and air pollution concentrations might vary by the degree of urbanicity, as mentioned in the introduction. However, other explanations are also plausible for the inconsistencies in the previous LUR models for the same study areas. First, government monitors with lower density in suburban/rural areas might not fully capture the relationship between spatial predictors and air pollution concentrations outside the urban cores. Second, the LUR models developed at different spatial scales were not always conducted at the same time, so the temporal changes in land use might contribute to the inconsistencies in the included spatial predictors. Other reasons include different techniques of model development (e.g., candidate buffers, predictor selection, treatment of missing values or outliers). Future studies will be needed to investigate whether the models in the urban cores and the corresponding larger metropolitan areas are different under the same processes of data collection and model development, and whether the differences in LUR models between urban cores and their metropolitan areas, if any, have an impact on health risk assessment at various spatial scales.

5. Conclusions

LUR models incorporating vertical variation were developed in Lanzhou urban core for $PM_{2.5}$ and NO_2. Substantial spatial variation was observed and explained by land use covariates, emphasizing the limitations of relying on government ambient monitors. Using the outputs of the LUR models might help to improve the accuracy of exposure assessment in future epidemiology studies. NO_2 and $PM_{2.5}$ concentrations showed different spatial patterns in the study area, indicating that investigating air pollutants at refined scale could potentially help disentangle the health effects of different pollutants or pollution sources. Furthermore, substantial vertical variations in pollutant levels by building height were observed in this study, and the vertical profiles differed by window directions and time of a day. More studies are needed to investigate how to incorporate vertical variations in exposure assessment, especially in study areas with dense high-rise residential buildings. The results of this study can potentially help the local government and the public to make informed decisions to control pollution and reduce exposures. Local government can make district-specific pollution control strategies based on the LUR predictions, prioritizing Qilihe District for $PM_{2.5}$ control, and Chengguan and Qilihe Districts for NO_2 control. Susceptible populations living in areas with high pollution levels can take protective measures to reduce exposures. Future epidemiology studies leveraging the LUR models' predictions are needed to investigate whether the observed fine-scale spatial variations and vertical variations of air pollution have health implications in Lanzhou.

Funding sources

This work was funded by Air & Waste Management Association, Yale MacMillan Center, Yale Institute for Biospheric Studies, Yale Hixon Center for Urban Ecology, Yale Tropical Resources Institute, Yale Global Health Initiative, Yale Graduate School, and Yale Council on East Asian Studies. This manuscript was developed under Assistance Agreement No. RD835871 awarded by the U.S. Environmental Protection Agency to Yale University. It has not been formally reviewed by EPA. The views expressed in this document are solely those of the authors and do not necessarily reflect those of the Agency. EPA does not endorse any products or commercial services mentioned in this publication. This manuscript was also developed under the Ministry of Science and Technology of the People's Republic of China grant 2016YFC1302500 and National Natural Science Foundation of China grant 21625701.

Declarations of interest

None.

Acknowledgment

We acknowledge Mr. Qiusheng Jin and Ms. Bei Zhang, who assisted Ms. Lan Jin with the field work. We acknowledge Dr. Jane Clougherty for lending Ogawa Badges, and Dr. Mikhail Wolfson and Dr. Marco Martins at Dr. Petros Koutrakis's lab for providing trainings and analyzing Ogawa pads. Funding for the fieldwork was provided by: Air & Waste Management Association, Yale MacMillan Center, Yale Institute for Biospheric Studies, Yale Hixon Center for Urban Ecology, Yale Tropical Resources Institute, Yale Global Health Initiative, Yale Graduate School, and Yale Council on East Asian Studies. This publication was developed under Assistance Agreement No. RD835871 awarded by the U.S. Environmental Protection Agency to Yale University. It has not been formally reviewed by EPA. The views expressed in this document are solely those of the authors and do not necessarily reflect those of the Agency. EPA does not endorse any products or commercial services mentioned in this publication. We also acknowledge the Ministry of Science and Technology of the People's Republic of China grant 2016YFC1302500, and National Natural Science Foundation of China grant 21625701.

Appendix A. Supplementary data

Supplementary data to this article can be found online at https://doi.org/10.1016/j.envres.2019.108597.

References

Apte, J.S., Messier, K.P., Gani, S., Brauer, M., Kirchstetter, T.W., Lunden, M.M., Marshall, J.D., Portier, C.J., Vermeulen, R.C.H., Hamburg, S.P., 2017. High-resolution air pollution mapping with google street view cars: exploiting big data. Environ. Sci. Technol. 51, 6999–7008.

Banerjee, S., Carlin, B., Gelfand, A., 2004. Hierarchical Modeling and Analysis for Spatial Data. Chapter 5, Hierarchical Modeling for Univariate Spatial Data.

Barratt, B., Lee, M., Wong, P., Tang, R., Tsui, T.H., Cheng, W., 2018. A Dynamic Three-Dimensional Air Pollution Exposure Model for Hong Kong. Research Report 194. Health Effects Institute, Boston, MA.

Beelen, R., Hoek, G., Pebesma, E., Vienneau, D., de Hoogh, K., Briggs, D.J., 2009. Mapping of background air pollution at a fine spatial scale across the European Union. Sci. Total Environ. 407, 1852–1867.

Beelen, R., Hoek, G., Vienneau, D., Eeftens, M., Dimakopoulou, K., Pedeli, X., Tsai, M.Y., Kunzli, N., Schikowski, T., Marcon, A., Eriksen, K.T., Raaschou-Nielsen, O., Stephanou, E., Patelarou, E., Lanki, T., Yli-Toumi, T., Declercq, C., Falq, G., Stempfelet, M., Birk, M., Cyrys, J., von Klot, S., Nador, G., Varro, M.J., Dedele, A., Grazuleviciene, R., Molter, A., Lindley, S., Madsen, C., Cesaroni, G., Ranzi, A., Badaloni, C., Hoffmann, B., Nonnemacher, M., Kraemer, U., Kuhlbusch, T., Cirach, M., de Nazelle, A., Nieuwenhuijsen, M., Bellander, T., Korek, M., Olsson, D., Stromgren, M., Dons, E., Jerrett, M., Fischer, P., Wang, M., Brunekreef, B., de Hoogh, K., 2013. Development of NO2 and NOx land use regression models for estimating air pollution exposure in 36 study areas in Europe - the ESCAPE project. Atmos. Environ. 72, 10–23.

Berman, J.D., Jin, L., Bell, M.L., Curriero, F.C., 2019. Developing a geostatistical simulation method to inform the quantity and placement of new monitors for a follow-up air sampling campaign. J. Expo. Sci. Environ. Epidemiol. 29, 248–257.

Chan, L.Y., Kwok, W.S., 2000. Vertical dispersion of suspended particulates in urban area of Hong Kong. Atmos. Environ. 34, 4403–4412.

Chen, G., Li, S., Knibbs, L.D., Hamm, N., Cao, W., Li, T., Guo, J., Ren, H., Abramson, M.J., Guo, Y., 2018a. A machine learning method to estimate PM 2.5 concentrations across China with remote sensing, meteorological and land use information. Sci. Total Environ. 636, 52–60.

Chen, L., 2010. GlobeLand30. http://www.globallandcover.com/home/Enbackground.aspx, Accessed date: 25 April 2019.

Chen, L., Bai, Z., Kong, S., Han, B., You, Y., Ding, X., Du, S., Liu, A., 2010a. A land use regression for predicting NO2 and PM10 concentrations in different seasons in Tianjin region, China. J. Environ. Sci. 22, 1364–1373.

Chen, L., Du, S.Y., Bai, Z.P., Kong, S.F., You, Y., Han, B., Han, D.W., Li, Z.Y., 2010b. Application of land use regression for estimating concentrations of major outdoor air pollutants in Jinan, China. J. Zhejiang Univ. - Sci. A 11, 857–867.

Chen, L., Gao, S., Zhang, H., Sun, Y., Ma, Z., Vedal, S., Mao, J., Bai, Z., 2018b. Spatiotemporal modeling of PM 2.5 concentrations at the national scale combining land use regression and Bayesian maximum entropy in China. Environ. Int. 116, 300–307.

Chu, P.C., Chen, Y.C., Lu, S.H., 2008. Atmospheric effects on winter SO2 pollution in Lanzhou, China. Atmos. Res. 89, 365–373.

Clougherty, J., Kheirbek, I., Eisl, H., Ross, Z., Pezeshki, G., Gorczynski, J., Johnson, S., Markowitz, S., Kass, D., Matte, T., 2013a. Intra-urban spatial variability in wintertime street-level concentrations of multiple combustion-related air pollutants: the New York city community Air survey (NYCCAS). J. Expo. Sci. Environ. Epidemiol. 23, 232–240.

Clougherty, J.E., Kheirbek, I., Eisl, H.M., Ross, Z., Pezeshki, G., Gorczynski, J.E., Johnson, S., Markowitz, S., Kass, D., Matte, T., 2013b. Intra-urban spatial variability in wintertime street-level concentrations of multiple combustion-related air pollutants: the New York City Community Air Survey (NYCCAS). J. Expo. Sci. Environ. Epidemiol. 23, 232–240.

Clougherty, J.E., Wright, R.J., Baxter, L.K., Levy, J.I., 2008. Land use regression modeling of intra-urban residential variability in multiple traffic-related air pollutants. Environ Health-Glob 7.

Cordioli, M., Pironi, C., De Munari, E., Marmiroli, N., Lauriola, P., Ranzi, A., 2017. Combining land use regression models and fixed site monitoring to reconstruct spatiotemporal variability of NO2 concentrations over a wide geographical area. Sci. Total Environ. 574, 1075–1084.

Demokritou, P., Kavouras, I.G., Ferguson, S.T., Koutrakis, P., 2001. Development and laboratory performance evaluation of a personal multipollutant sampler for simultaneous measurements of particulate and gaseous pollutants. Aerosol Sci. Technol. 35, 741–752.

Diggle, P., Ribeiro Jr., P., 2007. Model-based Geostatistics. Springer P134-154.

Eeftens, M., Beelen, R., de Hoogh, K., Bellander, T., Cesaroni, G., Cirach, M., Declercq, C., Dedele, A., Dons, E., de Nazelle, A., Dimakopoulou, K., Eriksen, K., Falq, G., Fischer, P., Galassi, C., Grazuleviciene, R., Heinrich, J., Hoffmann, B., Jerrett, M., Keidel, D., Korek, M., Lanki, T., Lindley, S., Madsen, C., Molter, A., Nador, G., Nieuwenhuijsen, M., Nonnemacher, M., Pedeli, X., Raaschou-Nielsen, O., Patelarou, E., Quass, U., Ranzi, A., Schindler, C., Stempfelet, M., Stephanou, E., Sugiri, D., Tsai, M.Y., Yli-Tuomi, T., Varro, M.J., Vienneau, D., von Klot, S., Wolf, K., Brunekreef, B., Hoek, G., 2012. Development of land use regression models for PM2.5, PM2.5 absorbance, PM10 and PMcoarse in 20 european study areas; results of the ESCAPE project. Environ. Sci. Technol. 46, 11195–11205.

Gaffin, J.M., Hauptman, M., Lai, P., Petty, C.R., Wolfson, J.M., Kang, C.M., Sheehan, W.J., Baxi, S.N., Bartnikas, L.M., Permaul, P., Gold, D.R., Coull, B., Koutrakis, P., Phipatanakul, W., 2017. Nitrogen dioxide exposure in School classrooms is associated with airflow obstruction in students with asthma. J. Allergy Clin. Immunol. 139 Ab174-Ab174.

GB3095-2012, 2012. Ambient air quality standards. http://extwprlegs1.fao.org/docs/pdf/chn136756.pdf, Accessed date: 10 April 2019.

Gilbert, N.L., Goldberg, M.S., Beckerman, B., Brook, J.R., Jerrett, M., 2005. Assessing spatial variability of ambient nitrogen dioxide in Montreal, Canada, with a land-use regression model. J. Air Waste Manag. Assoc. 55, 1059–1063.

He, B.H.Q., Heal, M.R., Reis, S., 2018. Land-use regression modelling of intra-urban air pollution variation in China: current status and future needs. Atmosphere-Basel 9.

He, Q., Huang, B., 2018. Satellite-based mapping of daily high-resolution ground PM2. 5 in China via space-time regression modeling. Remote Sens. Environ. 206, 72–83.

Henderson, S.B., Beckerman, B., Jerrett, M., Brauer, M., 2007. Application of land use regression to estimate long-term concentrations of traffic-related nitrogen oxides and fine particulate matter. Environ. Sci. Technol. 41, 2422–2428.

Ho, C.C., Chan, C.C., Cho, C.W., Lin, H.I., Lee, J.H., Wu, C.F., 2015. Land use regression modeling with vertical distribution measurements for fine particulate matter and elements in an urban area. Atmos. Environ. 104, 256–263.

Hoek, G., Beelen, R., de Hoogh, K., Vienneau, D., Gulliver, J., Fischer, P., Briggs, D., 2008. A review of land-use regression models to assess spatial variation of outdoor air pollution. Atmos. Environ. 42, 7561–7578.

Huang, L., Zhang, C., Bi, J., 2017. Development of land use regression models for PM2.5, SO2, NO2 and O-3 in Nanjing, China. Environ. Res. 158, 542–552.

James, G., Witten, D., Hastie, T., Tibshirani, R., 2013. An Introduction to Statistical Learning with Applications in R. Springer, pp. 101–102.

Jin, L., Berman, J.D., Zhang, Y., Thurston, G., Zhang, Y., Bell, M.L., 2019. Land Use Regression Study in Lanzhou, China: a Pilot Sampling and Spatial Characteristics of Pilot Sampling Sites. Atmospheric Environment.

Jun, C., Ban, Y., Li, S., 2014. China: open access to Earth land-cover map. Nature 514, 434.
Kanaroglou, P.S., Jerrett, M., Morrison, J., Beckerman, B., Arain, M.A., Gilbert, N.L., Brook, J.R., 2005. Establishing an air pollution monitoring network for intra-urban population exposure assessment: a location-allocation approach. Atmos. Environ. 39, 2399–2409.
Karner, A.A., Eisinger, D.S., Niemeier, D.A., 2010. Near-roadway air quality: synthesizing the findings from real-world data. Environ. Sci. Technol. 44, 5334–5344.
Larson, T., Henderson, S.B., Brauer, M., 2009. Mobile monitoring of particle light absorption coefficient in an urban area as a basis for land use regression. Environ. Sci. Technol. 43, 4672–4678.
Lee, J.H., Wu, C.F., Hoek, G., de Hoogh, K., Beelen, R., Brunekreef, B., Chan, C.C., 2014. Land use regression models for estimating individual NOx and NO2 exposures in a metropolis with a high density of traffic roads and population. Sci. Total Environ. 472, 1163–1171.
Lee, M., Brauer, M., Wong, P.L.N., Tang, R., Tsui, T.H., Choi, C., Cheng, W., Lai, P.C., Tian, L.W., Thach, T.Q., Allen, R., Barratt, B., 2017. Land use regression modelling of air pollution in high density high rise cities: a case study in Hong Kong. Sci. Total Environ. 592, 306–315.
Li, P., Deng, H., 2009. Blue Book Economic and Social Development in Lanzhou City. 2009-2010. Gansu Province People's Publishing House.
Li, X.L., Wang, J.S., Tu, X.D., Liu, W., Huang, Z., 2007. Vertical variations of particle number concentration and size distribution in a street canyon in Shanghai, China. Sci. Total Environ. 378, 306–316.
Lippmann, M., Cohen, B., Schlesinger, R., 2003. Environmental Health Sciences. Recognition, Evaluation, and Control of Chemical and Physical Health Hazards. Chapter 4 Dispersion of Contaminants. Oxford University Press.
Liu, S., Slaughter, J., Larson, T., 2002. Comparison of light scattering devices and impactors for particulate measurements in indoor, outdoor, and personal environments. Environ. Sci. Technol. 36, 2977–2986.
Liu, W., Li, X.D., Chen, Z., Zeng, G.M., Leon, T., Liang, J., Huang, G.H., Gao, Z.H., Jiao, S., He, X.X., Lai, M.Y., 2015. Land use regression models coupled with meteorology to model spatial and temporal variability of NO2 and PM10 in Changsha, China. Atmos. Environ. 116, 272–280.
Matte, T.D., Ross, Z., Kheirbek, I., Eisl, H., Johnson, S., Gorczynski, J.E., Kass, D., Markowitz, S., Pezeshki, G., Clougherty, J.E., 2013. Monitoring intraurban spatial patterns of multiple combustion air pollutants in New York City: design and implementation. J. Expo. Sci. Environ. Epidemiol. 23, 223–231.
Meng, X., Chen, L., Cai, J., Zou, B., Wu, C.F., Fu, Q., Zhang, Y., Liu, Y., Kan, H., 2015. A land use regression model for estimating the NO concentration in shanghai, China. Environ. Res. 137C, 308–315.
Qiu, X.H., Duan, L., Gao, J., Wang, S.L., Chai, F.H., Hu, J., Zhang, J.Q., Yun, Y.R., 2016. Chemical composition and source apportionment of PM10 and PM2.5 in different functional areas of Lanzhou, China. J Environ Sci-China 40, 75–83.
Quintana, P., Samimi, B., Kleinman, M., Liu, L., Soto, K., Warner, G., Bufalino, C., Valencia, J., Francis, D., Hovell, M., Delfino, R., 2000. Evaluation of a real-time passive particle monitor in fixed site residential indoor and ambient measurements. J. Expo. Anal. Environ. Epidemiol. 10, 437–445.
Rahman, M.M., Yeganeh, B., Clifford, S., Knibbs, L.D., Morawska, L., 2017. Development of a land use regression model for daily NO2 and NOx concentrations in the Brisbane metropolitan area, Australia. Environ. Model. Softw 95, 168–179.
Ribeiro Jr., P.J., Diggle, P.J., 2001. geoR: a package for geostatistical analysis. R. News 1 (No 2), 15–18 ISSN 1609-3631.
Ross, Z., English, P.B., Scalf, R., Gunier, R., Smorodinsky, S., Wall, S., Jerrett, M., 2006. Nitrogen dioxide prediction in Southern California using land use regression modeling: potential for environmental health analyses. J. Expo. Sci. Environ. Epidemiol. 16, 106–114.
Ross, Z., Ito, K., Johnson, S., Yee, M., Pezeshki, G., Clougherty, J., Savitz, D., Matte, T., 2013. Spatial and temporal estimation of air pollutants in New York City: exposure assignment for use in a birth outcomes study. Environ Health-Glob 12, 51.
Ross, Z., Jerrett, M., Ito, K., Tempalski, B., Thurston, G.D., 2007. A land use regression for predicting fine particulate matter concentrations in the New York City region. Atmos. Environ. 41, 2255–2269.
Shi, Y., Lau, K.K.L., Ng, E., 2016. Developing street-level PM2.5 and PM10 land use regression models in high-density Hong Kong with urban morphological factors. Environ. Sci. Technol. 50, 8178–8187.
Shi, Y., Lau, K.K.L., Ng, E., 2017. Incorporating wind availability into land use regression modelling of air quality in mountainous high-density urban environment. Environ. Res. 157, 17–29.
Vardoulakis, S., Gonzalez-Flesca, N., Fisher, B.E.A., 2002. Assessment of traffic-related air pollution in two street canyons in Paris: implications for exposure studies. Atmos. Environ. 36, 1025–1039.
Wolf, K., Cyrys, J., Harcinikova, T., Gua, J.W., Kusch, T., Hampel, R., Schneider, A., Peters, A., 2017. Land use regression modeling of ultrafine particles, ozone, nitrogen oxides and markers of particulate matter pollution in Augsburg, Germany. Sci. Total Environ. 579, 1531–1540.
Wu, J., Li, J., Peng, J., Li, W., Xu, G., Dong, C., 2015. Applying land use regression model to estimate spatial variation of PM2.5 in Beijing, China. Environ. Sci. Pollut. Res. Int. 22, 7045–7061.
Wu, C.D., MacNaughton, P., Melly, S., Lane, K., Adamkiewicz, G., Durant, J.L., Brugge, D., Spengler, J.D., 2014. Mapping the vertical distribution of population and particulate air pollution in a near-highway urban neighborhood: implications for exposure assessment. J. Expo. Sci. Environ. Epidemiol. 24, 297–304.
Wu, Y., Hao, J.M., Fu, L.X., Wang, Z.S., Tang, U., 2002. Vertical and horizontal profiles of airborne particulate matter near major roads in Macao, China. Atmos. Environ. 36, 4907–4918.
Xu, H., Bechle, M.J., Wang, M., Szpiro, A.A., Vedal, S., Bai, Y., Marshall, J.D., 2018. National PM2.5 and NO2 exposure models for China based on land use regression, satellite measurements, and universal kriging. Sci. Total Environ. 655, 423–433.
Yang, D., Lu, D., Xu, J., Ye, C., Zhao, J., Tian, G., Wang, X., Zhu, N., 2018. Predicting spatio-temporal concentrations of PM 2.5 using land use and meteorological data in Yangtze River Delta, China. Stoch. Environ. Res. Risk Assess. 32, 2445–2456.
Young, M.T., Bechle, M.J., Sampson, P.D., Szpiro, A.A., Marshall, J.D., Sheppard, L., Kaufman, J.D., 2016. Satellite-based NO2 and model validation in a national prediction model based on universal kriging and land-use regression. Environ. Sci. Technol. 50, 3686–3694.
Zhang, Q., Li, H.Y., 2011. A study of the relationship between air pollutants and inversion in the ABL over the city of Lanzhou. Adv. Atmos. Sci. 28, 879–886.
Zhang, Z., Wang, J., Hart, J.E., Laden, F., Zhao, C., Li, T., Zheng, P., Li, D., Ye, Z., Chen, K., 2018. National scale spatiotemporal land-use regression model for PM2. 5, PM10 and NO2 concentration in China. Atmos. Environ. 192, 48–54.